

ASSESSMENT AND MITIGATION OF THE PROTON-PROTON COLLISION DEBRIS IMPACT ON THE FCC TRIPLET

M. I. Besana*, F. Cerutti, S. Fartoukh, R. Martin¹, R. Tomas, CERN, Geneva, Switzerland
¹also at Humboldt University Berlin, Berlin, Germany

Abstract

The Future Circular hadron Collider (FCC-hh), which is designed to operate at a centre-of-mass energy of 100 TeV and to deliver ambitious targets in terms of both instantaneous and integrated luminosity, poses extreme challenges in terms of machine protection during operation and with respect to long-term damages. Energy deposition studies are a crucial ingredient for its design. One of the relevant radiation sources are collision debris particles, which deposit their energy in the interaction region elements and in particular in the superconducting magnet coils of the final focus triplet quadrupoles, to be protected from the risk of quenching and deterioration. In this contribution, the collision debris will be characterised and expectations obtained with FLUKA will be presented, including magnet lifetime considerations. New techniques including crossing angle gymnastics for peak dose deposition mitigation (as recently introduced in the framework of the LHC operation [1]), will be discussed.

INTRODUCTION

Proton-proton non-elastic collisions at 100 TeV centre-of-mass energy will direct a power of 43 kW towards each (Left/Right) side of the interaction point (IP) for the foreseen baseline instantaneous luminosity of $5 \cdot 10^{34} \text{ cm}^{-2} \text{ s}^{-1}$ [2], assuming a cross section of 108 mbarn; this is a factor of nine higher than what it is foreseen at the High-Luminosity LHC (HL-LHC). In each collision, about 210 secondary particles will be produced on average, with substantial fluctuations, as obtained from DPMJET-III [3] [4]. At 5 mm from the IP, the number increases by $\sim 30\%$ due to the decay of unstable particles and a clear prevalence of photons (almost one half) and charged pions (37%) is observed. Most of these particles are intercepted by the detector, releasing their energy within the experimental cavern. However, the most energetic ones, emitted at small angles with respect to the beam direction, travel farther in the beam pipe and reach the accelerator elements. In particular, charged particles are captured by the magnetic field and they cause a significant impact on the magnets along the interaction regions. The fraction of collision debris particles going through the Target Absorber Secondaries (TAS), the protection element in front of the final focus triplet on each side of the IP, is less than 5% of the total number¹, but they carry most of the total energy.

The energy deposition strongly depends on some key parameters, such as the magnet aperture, gradient and polarity,

* maria.ilaria.besana@cern.ch

¹ This is obtained, assuming a 3 m long TAS located between 31 m and 34 m from the IP, with 20 mm inner diameter aperture.

the crossing angle and the thickness of a shielding inside the cold bore [5]. Previous calculations [6], performed considering an inner triplet layout characterised by $L^*=36 \text{ m}$ (L^* being the distance between the IP and the first quadrupole) and a quadrupole coil aperture of 100 mm, have shown that the presence of shielding is mandatory. Without any shielding, the peak power density in the inner cable of the superconducting coils would reach 400 mW cm^{-3} , a factor of 10 higher than the expected quench limit for Nb₃Sn. The peak dose after the integrated luminosity of 3 ab^{-1} , which is expected to be already approached at end of the FCC-hh Phase I, would reach instead 3000 MGy, two orders of magnitude higher than the limit of 30 MGy assumed for LHC and HL-LHC. With a 5 mm thick tungsten shielding along the magnets and the interconnects², the peak power density decreases by more than an order of magnitude and with a 15 mm thick shielding it is further reduced down to 5 mW cm^{-3} . Analogous reduction factors apply to the dose.

INNER TRIPLET LAYOUT WITH $L^*=45 \text{ M}$

The first design of the FCC-hh detector [7] extends up to 31.5 m from the IP and it is characterised by the presence of a dipole in the forward region on each side of the IP. The effect of the detector spectrometer on the beam has to be corrected with a compensator dipole, put before the TAS. A new layout with a L^* value of 45 m has been therefore conceived, as shown in Fig. 1. Q1 and Q3 are focusing quadrupoles in the horizontal plane for positively charged particles and they have a length of 30.8 m, while Q2A and Q2B are defocusing and have a length of 26.4 m. These magnets feature a very large coil aperture: 205 mm (inner diameter) for Q1 and 248 mm for the others. The foreseen gradients are 107 T/m for Q1, 89 T/m for Q2A and Q2B and 86 T/m for Q3. A tungsten liner of 15 mm has been put along the magnets and the interconnects, with a tentative gap in each interconnect. The 3-m long TAS is located at a distance of 2 m from the Q1 front face and it has an aperture of 50 mm. The radiation calculations have been performed with FLUKA [8] [9] both for the case with the detector and compensator dipoles and the case without them, to compare with previous layouts.

Without Spectrometer and Compensator

Two optics configurations have been studied with half crossing angle of $89 \mu\text{rad}$, either in the vertical plane (v-crossing) or in the horizontal plane (h-crossing).

² The shielding is composed by INERMET180, which is a tungsten heavy alloy (W(95wt%)-Ni(3.5wt%)-Cu(1.5wt%)). A simplified hypothesis was considered at that stage, assuming a continuous shielding along both the magnets and the interconnects. This is an optimistic approximation, since the shielding in reality has some interruptions in the interconnects.

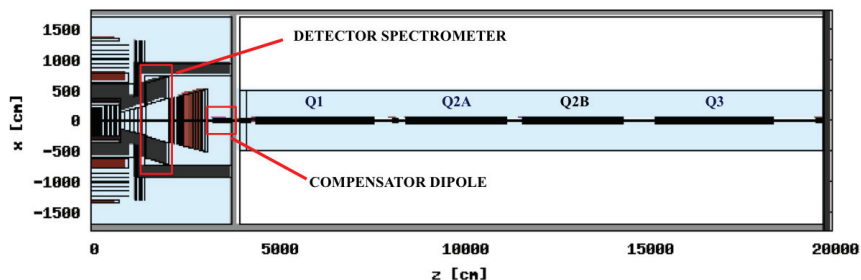


Figure 1: The interaction region layout on the right of the IP is shown up to the orbit corrector after the last inner triplet quadrupole. The detector components are modelled inside the experimental cavern on the left. The main magnets are indicated and the considered triplet polarity is FDDF in the horizontal plane, as explained in the text. The concrete (grey) walls extending beyond the cavern are not representative of the tunnel size.

The power absorbed by each inner triplet quadrupole is reported in Table 1, for the shielding and the cold mass separately. The maximum value on the cold mass is about 0.7 kW for Q1. The maximum peak power density on the magnet coils is at the end of Q1 and it reaches 2.5 mWcm^{-3} (2 mWcm^{-3}) for v-crossing (h-crossing), significantly below the expected quench limit.

Table 1: Total power in the four quadrupoles of the inner triplet for v-crossing and h-crossing, for the shielding and the cold mass separately.

	v-crossing [kW]		h-crossing [kW]	
	shielding	cold mass	shielding	cold mass
Q1	1.98	0.73	1.96	0.72
Q2A	0.34	0.23	0.33	0.13
Q2B	1.64	0.49	1.87	0.56
Q3	1.36	0.4	0.97	0.3

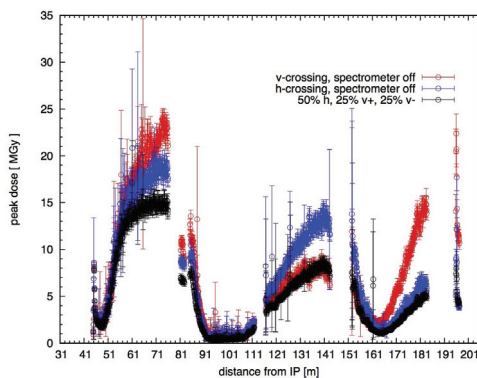


Figure 2: Peak dose in the coils for an integrated luminosity of 3 ab^{-1} as a function of z for v-crossing in red and for h-crossing in blue. The black curve has been obtained assuming to run 50% of the time in v-crossing (25% with an upward angle and 25% with a downward angle) and 50% in h-crossing. The error bars represent the statistical uncertainty.

Figure 2 shows the peak dose in the coils as a function of the longitudinal distance from the IP (z), for v-crossing in red and for h-crossing in blue. After 3 ab^{-1} , the maximum at

the end of Q1 is equal to 25 MGy and 20 MGy, respectively. This is 45% lower than what was obtained for the $L^*=36 \text{ m}$ case with a 15 mm thick shielding, thanks to the more than doubled magnet coil aperture (which in itself can be adjusted regardless of L^* , playing with the quadrupole gradient and corresponding length). The azimuthal position of the peaks is very well localised, reflecting in Q1 the crossing angle direction. This feature can be exploited by changing the crossing plane and the vertical angle polarity during the run, in order to share the maximum impact among different mid plane positions. The black curve in Fig. 2 has been obtained assuming to run 50% of the time in v-crossing (25% with an upward angle and 25% with a downward angle) and 50% in h-crossing³. The mixed scenario equalises the dose values at three azimuthal positions ($\pm \frac{\pi}{2}$ and 0) and reduces the maximum down to 15 MGy, yielding a lifetime increase of 60% with respect to the worse fixed angle case (v-crossing).

With Spectrometer and Compensator

The detector spectrometer is assumed to give the beam a horizontal kick of $60 \mu\text{rad}$. The compensator dipole is a 4.5 m long warm magnet inside the experimental cavern with a large coil aperture of 165 mm, to prevent undesired backscattering to the detector. The magnetic field is 1.5 T, providing an opposite kick of $42 \mu\text{rad}$. This gives an additional half crossing angle of $18 \mu\text{rad}$ on the horizontal plane, which combines with the external angle. For the latter, also this layout has been analysed considering both schemes. In h-crossing, the worse case for energy deposition is obtained when the experiment angle has the same sign as the external one, maximising the internal horizontal crossing angle at the IP, which here turns out to equal $110 \mu\text{rad}$. In v-crossing, we assumed that the experiment horizontal angle is cancelled by external correction and we were left with a purely vertical internal half crossing angle of $85 \mu\text{rad}$.

Because of the effect of the dipole fields, the peak dose profile along the triplet changes and the maximum value reaches 30 MGy for h-crossing (with unfavourable spectrometer polarity) and 28 MGy for v-crossing, as it can be seen in Fig. 3.

³ In the case of horizontal crossing the sign of the angle has no degree of freedom, to avoid undesired bunch collisions in the machine by the separation dipole following the triplet at a larger distance from the IP.

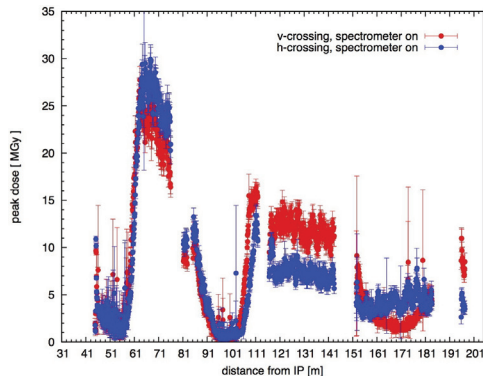


Figure 3: Peak dose in the coils for an integrated luminosity of 3 ab^{-1} as a function of z , for v-crossing in red and for h-crossing in blue, in the presence of the spectrometer and compensator dipoles.

Figure 4 shows the dose distribution in the innermost strands of the magnet coils as a function of z and of the azimuthal angle, for v-crossing. Contrary to the case without dipoles, the peak dose at the end of Q1 is on the horizontal plane (here at $\Phi = \pm\pi$, while it would be at $\Phi = 0$ for opposite spectrometer polarity), as for h-crossing. This peak is due to negatively charged pions that are deflected in the horizontal plane by the combined effect of the spectrometer and of the field in Q1. The number of negative pions captured in Q1

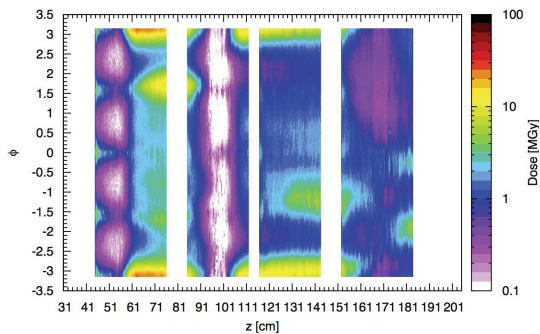


Figure 4: Dose distribution averaged over the innermost 3 mm of the magnet coil, as a function of z and of the azimuthal angle, normalised to an integrated luminosity of 3 ab^{-1} . It refers to v-crossing, in the presence of the detector spectrometer and the compensator dipole.

is in fact significantly higher than the respective number of positive pions and protons, as it can be seen comparing the area between the pink and red curves in the three frames of Fig. 5. The peak dose at the end of Q2A and in Q2B is in the same angular position, but it is due to positively charged particles.

Apart from regular switching of the spectrometer and compensator polarity, the external crossing scheme as well as the triplet polarity offer additional degrees of freedom to mitigate the maximum dose. The effectiveness of these measures will be subject of further studies.

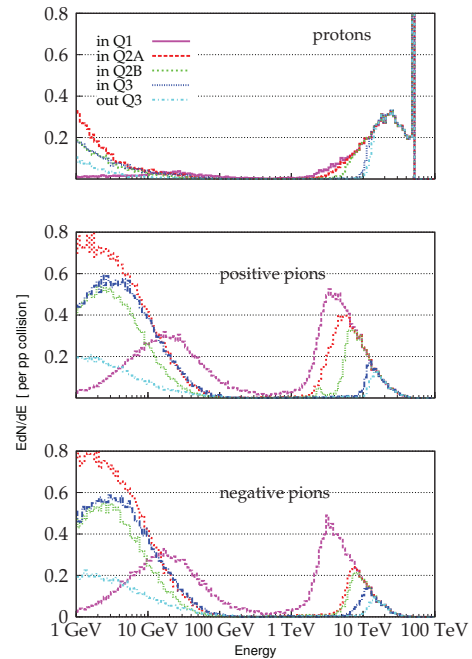


Figure 5: Spectra of protons [top], positively charged pions [middle] and negatively charged pions [bottom] in the inner triplet vacuum chamber are shown at the entrance (in) of the four quadrupoles and at the exit (out) of the last. They refer to v-crossing, in the presence of the spectrometer and the compensator and are normalised to one proton-proton collision. The number of particles captured in a given magnet is equal to the difference between their high energy spectrum at the entrance of the magnet itself and their high energy spectrum at the entrance of the following element. Low energy tails are populated by reinteraction products.

CONCLUSIONS

A new optics and interaction region layout with $L^* = 45 \text{ m}$ have been designed to fit the proposed detector model. They feature a very large quadrupole coil aperture, allowing to keep the maximum dose absorbed by the superconducting cables at $40 \text{ MGy per } 5 \text{ ab}^{-1}$ with 15mm tungsten shielding, for v-crossing at fixed angle (lower at 33 MGy for h-crossing), provided a suitable extension of the absorber in the interconnections is guaranteed. Regular crossing plane and vertical angle polarity alternation are found to reduce the maximum dose to 25 MGy in both high luminosity insertions, yielding a 60% lifetime increase. Irrespective of the adopted magnet aperture and corresponding absolute dose values, such a gymnastics has the potential of assuring a considerable gain, to be optimized according to the specific layout features. In particular, the presence of the detector spectrometer changes the picture, but it does not drastically alter the relevant values, opening at the same time to the possible exploitation of several degrees of freedom (experiment angle polarity, external crossing scheme and triplet polarity).

REFERENCES

- [1] S. Fartoukh *et al.*, “LHC triplet lifetime versus operational scenario in ATLAS and CMS”, presented at the 225th LHC Machine Committee, 8 July 2015, https://indico.cern.ch/event/406858/contributions/966580/attachments/813759/1115141/LMC_IR1sign.pdf
- [2] D. Schulte, “Preliminary collider baseline parameters”, EuroCirCol-D1-1, 2015g.
- [3] S. Roesler, R. Engel, and J. Ranft, “The Monte Carlo event generator DPMJET-III”, in *Proc. Monte Carlo 2000 Conference*, Lisbon, Portugal, Oct. 2000, A. Kling, F. Barao, M. Nakagawa, L. Tavora, P. Vaz eds., Springer-Verlag Berlin, pp. 1033-1038, 2001.
- [4] A. Fedynitch and R. Engel, “Revision of the high energy hadronic interaction models PHOJET/DPMJETIII”, in *Proc. 14th International Conference on Nuclear Reaction Mechanisms*, Varenna, Italy, Jun. 2015 edited by F. Cerutti, M. Chadwick, A. Ferrari, T. Kawano and P. Schoofs, CERN Proceedings-2015-001 (CERN, Geneva, 2015), pp. 291-299, <https://cds.cern.ch/record/2114737>.
- [5] R. Martin, M. I. Besana, F. Cerutti, and R. Tomas, “Radiation load optimization in the final focus system of FCC-hh”, presented at the 7th Int. Particle Accelerator Conf. (IPAC’16), Busan, Korea, May 2016, paper TUPMW018.
- [6] M. I. Besana *et al.*, “Beam losses and collision debris studies in Europe”, presented at the First Annual Meeting of the Future Circular Collider study, http://indico.cern.ch/event/340703/contributions/802261/attachments/668837/919365/FCCweek_MIBesana.pdf
- [7] M. I. Besana, F. Cerutti, A. Ferrari, W. Riegler, and V. Vlachoudis “Characterization of the Radiation Field in the FCC-hh Detector”, presented at the 7th Int. Particle Accelerator Conf. (IPAC’16), Busan, Korea, May 2016, paper TUPMW005.
- [8] A. Ferrari, P.R. Sala, A. Fassò, and J. Ranft, “FLUKA: a multi-particle transport code”, Rep. CERN-2005-10, INFN/TC 05/11, SLAC-R-773, Oct. 2005.
- [9] G. Battistoni *et al.*, “Overview of the FLUKA code”, *Annals of Nuclear Energy*, vol. 82, pp. 10-18, Aug. 2015.